EXPERIMENTS WITH THE MESONH-AROME MICROPHYSICAL SCHEME AND EVALUATION BY REMOTE SENSING TOOLS

Jean-Pierre Pinty(*), Jean-Pierre Chaboureau(*),
Evelyne Richard(*), Frank Lascaux(*) and Yann Seity(**)

(*) Laboratoire d'Aérologie, Observatoire Midi-Pyrénées, Toulouse, France
(**) Météo-France, Toulouse, France

1. INTRODUCTION

The trend is now to develop new operational forecast systems for scales much lower than 10 km in order to better resolve mesoscale flows such as breezes, isolated storms, orographic flows and organized convective systems. Some of these projects, the Unified Model (UK MetOffice), the Local Model (DWD, Germany), WRF (NCAR-NOAA, USA), AROME (Météo-France), ALARO (ALADIN community), have already incorporated advanced features in NWP models. Among these are non-hydrostatic dynamics cores, turbulence schemes with 3D capabilities and multi phase microphysical schemes. Here we focus on the explicit resolution of clouds and precipitation at a few km scale for which standard and sometimes sophisticated microphysical schemes currently used in research mesoscale models could be adapted for NWP purpose.

Many operational NWP systems employ several techniques, semi-Lagrangian and semi-implicit numerical schemes or variational data assimilation schemes, which are far less popular in mesoscale models. This leads to new aspects in explicit cloud modeling. For the numerics, the traditional explicit, conservative, positive definite schemes tend to be substituted by two time level robust schemes to perform the temporal integration with large time steps. This question is crucial for the treatment of the sedimentation fluxes of precipitation which may fall from several levels in a single time step. Another debate is the desirable initialization of the water cycle in order to reduce the model spin up in the formation of cloud fields. Assimilation of cloudy satellite radiances and radar data is known to be a strong issue to obtain high resolution analyses of the cloud and humidity fields. Last, the development of verifying tools and the definition of new scores to appreciate the quality of nebulosity and ground precipitation forecasts are also foreseen.

Corresponding author's address: Jean-Pierre Pinty, Lab. Aérologie, OMP, 14 av. E. Belin, 31400, Toulouse, France; e-mail <pinjp@aero.obs-mip.fr>.

2. EXPLICIT CLOUD MODELING

2.1 Generalities

The clouds are at the origin of many interactions with the dynamics, the radiation, the surface properties, the aerosols, the chemistry and the atmospheric electricity. There are many cloud types to simulate. The fogs, the extended warm cloud sheets, the cirrus, the cumulus and the heavily precipitating clouds contain a wide range of particle size and particle habit. A numerical difficulty arises because the microphysical fields are sparse and discontinuous with sharp cloud boundaries. So it is important to realize that simulating the localization and persistence of the clouds and the generation of precipitation is still a difficult task.

A key-question in cloud modeling turns around the optimal number of different ice species to carry out and the way, number concentrations should be described. It is now commonly accepted that mixing ratios (mass of water scaled by the mass of dry air) lead to the simplest equations of conservation of the water substance. As the prediction of number concentrations critically depends on yet poorly known aerosol properties (activation and nucleation) this issue seems out of reach to NWP models for the moment. Most of mixed-phase microphysical schemes consider two variables for the water (cloud droplets and rain drops) and three variables for the ice phase (small ice crystals, unrimed or aggregated large crystals and a graupel, frozen rain, hail mixed category). Other combinations, including a separate prediction of snow and hail, have been also advocated as well as simplified schemes with a single non-precipitating and precipitating category of water but with additional assumptions.

Besides a limited number of water species, the microphysical schemes share many common features. The size distribution of the particles are described by a continuous parametric distribution law in the $0 < D < \infty$ range, where D is a characteristic dimension (diameter of water drops). The mass-size and fall speed-size relationships are simple enough to enable analytical integrations. However all the

schemes suffer from uncertainies about bulk coefficients and about the representation of some processes. For example, the collision-sticking efficiencies of the collection kernels of ice-ice interactions are poorly known. Many questions concern the treatment of the autoconversion processes that govern the onset of precipitating particles. The common practice of adjustment to saturation in mixed-phase clouds is also questionable.

2.2 The MESONH microphysical scheme

In its essence, the MESONH scheme follows the approach of Lin et al. (1983) that is a three-class ice parameterization coupled to a Kessler's scheme for the warm processes. The scheme predicts the evolution of the mixing ratios of six water species: r_v (vapor), r_c and r_r (cloud droplets and rain drops) and r_i, r_s and r_g (pristine ice, snow/aggregates and frozen drops/graupels defined by an increasing degree of riming). The concentration of the precipitating particles is parameterized as in Pinty and Jabouille (1998) with a total number $N = C\lambda^x$. λ is the slope parameter of the size distribution, C and x are empirical ajustments drawn from observations. The size distribution of the hydrometeors follows a generalized Gamma distribution:

$$n(D)dD = Ng(D)dD = N\frac{\alpha}{\Gamma(\nu)}\lambda^{\alpha\nu}D^{\alpha\nu-1}exp\big(-(\lambda D)^{\alpha}\big)dD \quad (1)$$

where $g(D)$ is the normalized distribution while ν and α, ajustable parameters ($\nu = \alpha = 1$ gives the Marshall-Palmer distribution law). Finally, suitable power laws are taken for the mass-size ($m = aD^b$) and for the velocity-size ($v = cD^d$) to perform useful analytical integrations using the moment formula:

$$M(p) = \int_0^{\infty} D^p g(D)dD = \frac{\Gamma(\nu + p/\alpha)}{\Gamma(\nu)}\frac{1}{\lambda^p}, \quad (2)$$

where $M(p)$ is the p^{th} moment of $g(D)$. A first application of (2) is to compute the mixing ratio $\rho r_x = aNM_x(b)$, where ρ is the air density. Table 1 provides the complete characterization of each ice categories and of the cloud droplets/raindrops.

The microphysical scheme is sketched in Diagram 1 where the colored boxes represent the different category of water substance. The pristine ice category is initiated by homogeneous nucleation (**HON**) when T$\leq -35^o$C, or more frequently by heterogeneous nucleation (**HEN**, the small ice crystal concentration is a simple function of the local supersaturation over ice). These crystals grow by water vapor deposition (**DEP**, see below) and by the Bergeron-Findeisen effect (**BER**). The snow phase is initiated by autoconversion (**AUT**) of the primary ice crystals; it grows by deposition (**DEP**) of water vapor, by aggregation (**AGG**) through small crystal collection and by the light riming produced by impaction of cloud droplets (**RIM**) and of raindrops (**ACC**). The graupels are produced by the heavy riming of snow (**RIM** and **ACC**) or by rain freezing (**CFR**) when supercooled raindrops come in contact with pristine ice crystals. According to the heat balance equation and to the efficicency of their collecting capacity, graupels can grow either in the (**DRY**) mode or in the (**WET**) mode when riming is very intense (as for hailstone embryos). In the latter case, the excess of non-freezable liquid water at the surface of the graupels is shed (**SHD**) and evacuated to form raindrops. When T$\geq$ 0^{o}C, pristine crystals immediately melt into cloud droplets (**MLT**) while snowflakes are progressively converted (**CVM**) into graupels that melt (**MLT**) as they fall. The other processes are those described by the Kessler scheme: autoconversion of cloud droplets (**AUT**), accretion (**ACC**) and rain evaporation (**EVA**). Cloud droplets excepted, each condensed water species has a substantial fall speed so giving an integrated sedimentation rate (**SED**).

	r_i	r_s	r_g	r_c	r_r
α	3	1	1	3	1
ν	3	1	1	3	1
a	0.82	0.02	19.6	524	524
b	2.5	1.9	2.8	3	3
c	800	5.1	124	3.2 10^7	842
d	1.00	0.27	0.66	2	0.8
C		5	5 10^5		10^7
x		1	-0.5		-1

Table 1: Characteristics of water-ice categories.

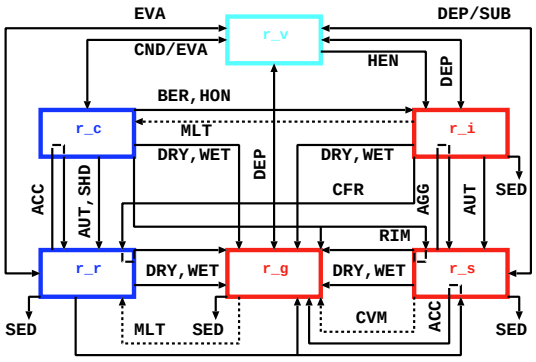

Diagram 1: Processes in the mixed-phase scheme.

The possible coexistence of cloud droplets and small ice crystals in mixed-phase clouds necessitates a careful treatment of the fast water vapor exchanges (**DEP** and **CND**). As is usually done, the "floating" water vapor saturation pressure $r_{v_{c,i}}^{sat}$, is defined

by a barycentric formula using the vapor saturation curves over water and ice and the mass amounts r_c and r_i, respectively. In the parameterization, the **DEP** and **CND** terms result from an implicit adjustment relative to $r_{v_{c,i}}^{sat}$, but with an original closure where any deficit/excess of r_v due to the adjustment, is compensated/absorbed by each condensed phase in proportion to its actual amount. The algorithm is non-iterative and 2nd order accurate.

The other processes that need a special attention are the collection processes. When non (r_c) or very slowly (r_i) precipitating categories are involved, the collection rates are computed analytically using the geometric sweep-out concept of the collection kernels defined for the large collecting particles (raindrops, snowflakes or graupels). When both interacting particles are precipitating, an analytical integration over the spectra is no longer possible and pre-tabulated kernels are used. For each ice-ice interaction, a major point of concern is the tuning of the sticking efficiencies which are still poorly understood functions of the temperature in most cases. After a series of experiments, the last set of coefficients retained by Ferrier et al. (1995) has been adopted. Finally, the microphysical processes are integrated one by one after carefully checking the availability of the sinking categories.

The detailed documentation of the scheme can be obtained at http://aero.obs-mip.fr/mesonh/.

3. EXAMPLES WITH MESONH/AROME

3.1 Generalities

MESONH is a multi-purpose non-hydrostatic anelastic mesoscale model, jointly developed by Météo-France and Laboratoire d'Aérologie (Lafore et al., 1998). It contains multiscale physical parameterizations to simulate academic and real flows with the grid-nesting technique. In addition and in order to facilitate the comparison between observations and model results, many diagnostics such as radar reflectivities or satellite images are available. This section illustrates the behaviour of the microphysical scheme of MESONH for real flow studies.

3.2 The Gard flash flood experiment

The Gard flash flood event that occurred in the South of France on Sept. 8th 2002 was very devastating. A peak of 300 mm of accumulated precipitation was recorded by the Nîmes radar between 12-22 UTC (see Fig. 1a). The heavy rainfall found there are the result of a southerly flow over the Gulf of Lions (Mediterranean sea) which is forced to lift because of the Cevennes ridge in the south edge of the Massif Central. Obviously, there is a strong interest to simulate this extreme event at high resolution.

Several numerical experiments are performed for this case study. Best results are obtained using ARPEGE analyses and additional mesoscale observations, such as mesonet surface observations, radar reflectivities, and Meteosat data (Ducrocq et al., 2002). Fig. 1b shows the cumulated rainfall as simulated by MESONH with a double grid nesting at 10 km and 2.5 km horizontal resolution. The boundary conditions are provided by 3 hour ALADIN forecasts. The comparison with the radar derived cumulated rainfall (Fig. 1a) shows a good agreement for the location of the precipitating area and a slight underestimation of the peak value. Previous experiments indicate that the relatively high quality of the present simulation is mostly due to the enhanced analyses at high resolution.

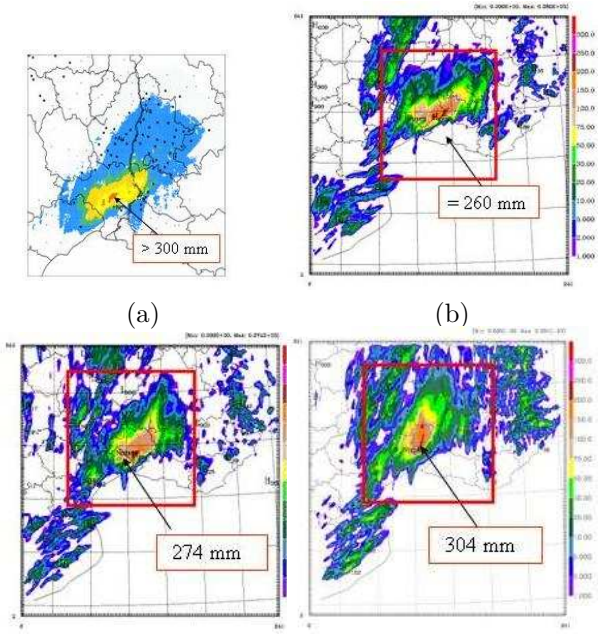

Figure 1: Gard experiment: a) 12-22 UTC Nîmes radar cumulated rainfall, b) MESONH with grid-nesting, c) MESONH as single model, d) AROME, 2.5 km simulations.

For comparison purpose, the simulation is redone by MESONH with a timestep of 4 s. but without grid-nesting and by an AROME prototype allowing for a larger timestep (60 s.). Both models are initialized the same way and run at 2.5 km resolution. For short the AROME version is based on the ALADIN dynamics but incorporates the physical package of MESONH without modification. Results are shown in Fig. 1c and 1d. The differences between the two MESONH simulations (Figs 1b and 1c) are attributed to the grid nesting. The first simulation performs slightly better for the location of the precipitating area while the peak value is improved in the second one. The AROME results shown in Fig. 1d compare reasonnably well with those of MESONH but the orientation of the

rainy area pattern seems less accurate. A conclusion drawn from this test is that the microphysical scheme of MESONH is rather flexible and can be integrated with large timesteps as compared to the usual practice.

3.3 The "MAP" orographic precipitation

The MAP experiment was set up to study the flow across, above, around the Alpine bow and to relate the precipitation patterns to the fine scale orography (Bougeault et al. 2001). A field experiment with Intensive Observing Periods (IOP) took place during fall 1999 for which many numerical simulations were performed to evaluate quantitative precipitation forecasts at high resolution. The 2 km simulation domain shown in Fig. 2, encompasses the north of Italy and the south of Switzerland.

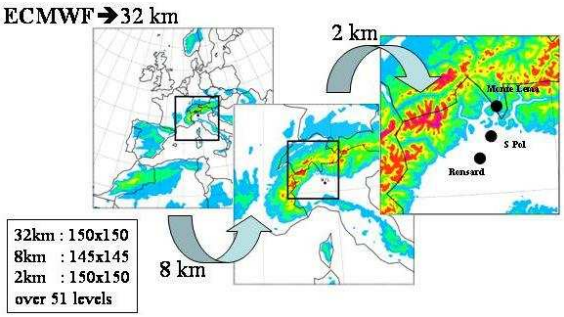

Figure 2: Configuration of MESONH for 3 level grid-nested simulations of MAP. Dots indicate radar locations.

Fig. 3 shows results obtained for the simulation of IOP2a at 2 km resolution. MESONH is initialized and takes boundary conditions from ECMWF analyses at 32 km. The simulation starts on sept. 17th 1999 at 12 UTC. At the end of the afternoon, a major squall line formed on the foothills of the southeastward facing slopes of the Lago Maggiore region in Italy and intensified during its propagation to the east as a three-dimensional convective cluster (Richard et al., 2003). This intense orogenic system with lots of lightning impacts and precipitation amounts of more than 70 mm in 6 hours, was well observed by the three radars. Two twin experiments are performed with MESONH for this case. In the first one, the standard microphysical scheme of MESONH is used while in the second one, an explicit hail category of ice is added. In the latter case, the formation of hail particles is derived from the **WET** and **DRY** growth modes of the graupels. Once formed hail grows exclusively in the **WET** growth mode. No reverse conversion to the graupel category is possible. Hailstones fall and melt into rain at a rate which is explicitly computed.

Examination of the radar reflectivity fields in Fig. 3 suggests that MESONH is able to timely capture the formation and displacement of the convective system (similar "horseshoe" pattern at $z = 2000$ m). Indeed it seems that considering hail as a fourth category of ice is beneficial in this case, at least to reproduce the high reflectivity cores at $z = 6000$ m.

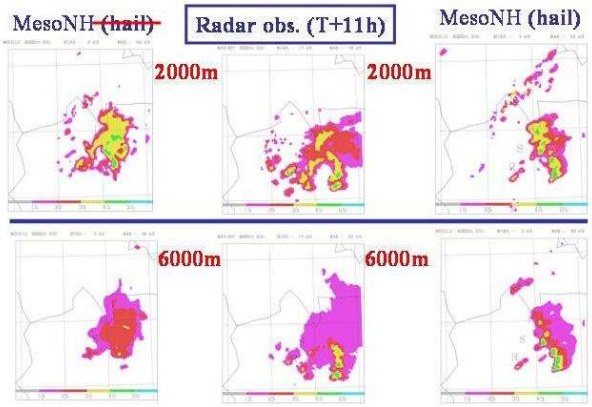

Figure 3: Radar reflectivity maps at $z = 2000$ m (top) and at $z = 6000$ m (bottom). Data are in the central column.

In order to illustrate the variable distribution of microphysical species on the vertical, the mixing ratios are averaged on the horizontal over the rainy areas. The left plot in Fig. 4 (IOP2a case) shows that the 1D profiles are those of deep convective clouds topping at 12 km with a remarkable stratification. The lightest particles (cloud ice) are aloft while the densiest ones (hail) are peaking at 4 km high and even can reach the ground. The IOP2a vigorous convection case of MAP is in contrast with the IOP8 case showing a shallower precipitating system. In the IOP8 case on the right side of Fig. 4, snow is the dominant type of ice particle as in stratiform systems. These MAP numerical simulations let us to conclude that the microphysical scheme of MESONH is able to simulate very different types of precipitating clouds forming on the same area.

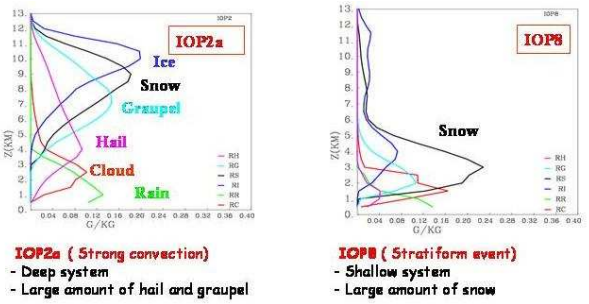

Figure 4: 1D vertical profiles of the horizontally averaged mixing ratios of IOP2a (left) and IOP8 (right) MAP cases.

3.4 Storms over Germany on Aug 12th 2004

MESONH is used to study a moving deep convective system which intensifies over the south of Germany. The simulation is performed with three

grid-nested models running at 40, 10 and 2.5 km resolution, respectively. Model results at 10 km scale are shown in Fig. 5. The purpose of this case study is to illustrate how multichannel satellite observations can be very powerful to pertain the quality of a simulation. The top row of Fig. 5 corresponds to satellite images with in order, the brightness temperature (BT) of the SEVIRI (MSG) 10.8 μm IR channel, a BT difference between 10.8 μm and 12 μm (the split window technique to show up cirrus clouds) and the coincident microwave temperature at 183 ± 1 GHz from AMSUB (NOAA15). As far as clouds are concerned, the plots picture the cloud top temperature, then the extent and opacity of high level clouds and finally the amount of large scattering particles of ice. The second row of Fig. 5 provides the corresponding simulation results obtained with the fast radiative transfer code RTTOV-7 (Saunders et al., 2002) using MESONH outputs valid for the same time 17 UTC (the simulation started at 00 UTC from the ECMWF analysis).

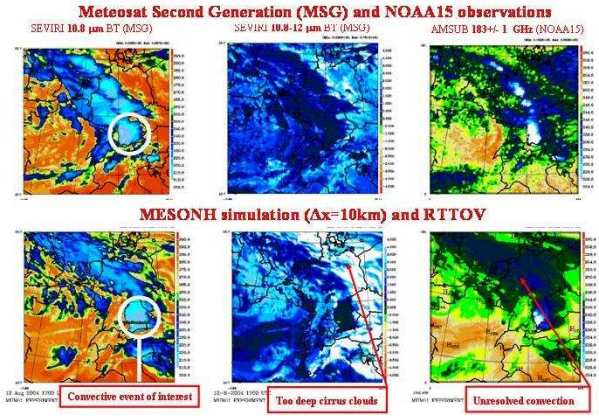

Figure 5: Satellite pictures from MSG and NOAA 15 (top row) and MESONH outputs with RTTOV (bottom row).

The first column of Fig.5 shows that the convective event of interest (circled in white) is well captured by MESONH. The high resolution model at 2.5 km is centered over this area. It is the feedback from this model to the 10 km one (two-way grid-nesting) which brings a significant contribution to the cloud field since at 10 km scale, most of the convection comes from the deep convection scheme. The central column reveals a biais of bright ΔTB in MESONH suggesting that the model tends to produce too much ice in the upper levels. This feature can be easily circumvented by readjusting the ice autoconversion parameterization as shown by Chaboureau et al. (2002). The last column of Fig. 5 provides an indication of the presence of large ice particles, snow or graupel. The detection of these particles is efficient for the part of storm over the south of Germany. However the bright spots tracing the convective bow in the AMSUB data are not present in the picture deduced from MESONH. The reason is again that convection is not explicitly resolved so without feedback from a high resolution model at these locations, the amount of snow and graupel is poorly estimated. The unresolved clouds of the deep convection scheme are transparent in our RTTOV-7 implementation for the moment.

4. CONCLUSION

The study reports results obtained with the microphysical scheme developped in the French mesoscale model MESONH. Several meteorogical cases are simulated at high resolution, down to the 2 km scale. The results show that the microphysical scheme coupled to MESONH or to AROME is able to capture an extreme precipitating event. Other experiments made for a variety of precipitating systems over orography and for a deep convective event confirm the benefit of explicit cloud modeling. The last point to mention is that many data are now available from ground radars and spaceborne sensors. In this context, the extensive use of these data is the coming step in explicit cloud modeling.

5. REFERENCES

Bougeault, P., P. Binder, A. Buzzi, R. Dirks, R. Houze, J. Kuettner, R. B. Smith, R. Steinacker, H. Volkert and all the MAP scientists, 2001: The MAP special observing period.*Bull. Am. Meteor. Soc.,* **82**, 433-462.

Chaboureau, J.-P., J.-P. Cammas, P. J. Mascart, J.-P. Pinty, and J.-P. Lafore, 2002: Mesoscale model cloud scheme assessment using satellite observations, *J. Geophys. Res.*, 107(D16), 4301, doi:10.1029/2001JD000714.

Ducrocq, V., D. Ricard, J.-P. Lafore, and F. Orain, 2002: Storm-scale numerical rainfall prediction for five precipitating events over France: On the importance of the initial humidity field, *Wea. Forecasting*, 17, 1236-1256.

Ferrier, B. S., W.-K. Tao, and J. Simpson, 1995: A double-moment multiple-phase four-class bulk ice scheme. Part II: Simulations of convective storms in different large-scale environments and comparisons with other bulk parameterizations. *J. Atmos. Sci.,* **52**, 1001-1033.

Lafore, J.-P. et al., 1998: The Meso-NH Atmospheric Simulation System. Part I: adiabatic formulation and control simulations. Scientific objectives and experimental design, *Ann. Geophys.*, 16, 90-109.

Lin, Y.-L., R. D. Farley, and H. D. Orville, 1983: Bulk parameterization of the snow field in a cloud model. *J. Climate Appl. Meteor.,* **22**, 1065-1092.

Pinty, J.-P. and P. Jabouille, 1998: A mixed-phase cloud parameterization for use in a mesoscale non-hydrostatic model: simulations of a squall line and of orographic precipitation. In *Conf. on Cloud Physics*, Everett, WA. Amer. Meteor. Soc., 217-220.

Richard, E., S. Cosma, P. Tabary, J.-P. Pinty, and M. Hagen, 2003: High-resolution numerical simulations of the convective system observed in the Lago Maggiore area on 17 September 1999 (MAP IOP 2a), *Quart. J. Roy. Meteor. Soc.*, 129, 543-563.

Saunders, R., Brunel P., Chevallier F., Deblonde G., English S., Matricardi M., and Rayer P., 2002: RTTOV-7 science and validation report. Met Office Tech. Rep. FR-387, 51 pp.